Proceedings of the Second International Conference on Press-in Engineering 2021, Kochi, Japan – Matsumoto et al (eds)

Study on liquefaction countermeasure method of river embankment using wood and sheet pile

G. Hashimura, K. Okabayashi & D. Yoshikado
National Institute of Technology, Kochi College, Nankoku City, Kochi, Japan

Y. Kajita
Chiyoda Engineering Consultants Co., Ltd, Chiyoda Ward, Tokyo, Japan

ABSTRACT: In this study, the construction method using wooden piles and steel sheet piles was examined as a countermeasure against liquefaction of river embankments. The behavior of river levees was confirmed, and the effect of countermeasures was evaluated in each of the models.
As the research method, liquefaction experiments using a dynamic centrifuge and analysis using effective stress analysis (LIQCA) were performed.
As a result, with no measures taken, the lateral flow due to liquefaction occurred on the horizontal ground on both sides of the river embankment and the embankment subsided.
In the case where countermeasures were taken, displacement of the embankment could be suppressed. By penetrating the wooden piles, the ground density increased, and the effect of liquefaction countermeasures was obtained. Also, it was confirmed that the deformation of the embankment and the lateral flow was suppressed by penetrating the steel sheet piles.

1 INTRODUCTION

The 2011 off the Pacific coast of Tohoku Earthquake caused large-scale levee damage along the river coasts. According to a survey by the Ministry of Land, Infrastructure, Transport, and Tourism (2011), a total of 1195 damages were confirmed in 5 of the 12 water systems managed by the Tohoku Regional Development Bureau on the Pacific Oceanside. Also, the main cause of the levee damage in the upstream area was levee settlement due to liquefaction of the ground.

In the Nankai Trough, located off the coast of Kochi Prefecture, the probability of an earthquake occurring in the next 30 years is 70 to 80% (Japan Meteorological Agency (2020)). According to the assumption of Kochi Prefecture (2013), it is said that land settlement due to liquefaction will occur mainly in Kochi City, and it is predicted that the damage caused by the run-up of the tsunami will increase due to the loss of the levee function.

The purpose of this study is to consider and propose a liquefaction countermeasure construction method for river embankments, the effect of liquefaction countermeasures on river embankments due to the penetration of wooden piles and steel sheet piles will be examined. The wooden piles aim at suppressing liquefaction by increasing the ground density, and the steel sheet piles aim at suppressing the deformation of river embankments. The method of increasing the ground density using wooden piles is expected to have the effect of suppressing liquefaction. The construction method was used when actually constructing the new Kochi City Government Building (Kochi City (2015)). The application of this method to the river embankment is examined. Also, various studies have already been conducted on the construction method using steel sheet piles in the embankment structure. In our laboratory, the effectiveness had been examined from the viewpoint of the penetration depth of steel sheet piles (Nakazawa (2018)). In this study, we focus on the construction position of the steel sheet pile and examine the effect of countermeasures. It is compared to the results of the experiment and analyzed to confirm the suitability. Besides, the effectiveness of each liquefaction countermeasure method is examined.

2 RESEARCH METHOD

2.1 *Research case*

Figure 1 shows the study model. In this study, we examine five models (Case1: Unmeasured model with only embankment constructed, Case2: 4m

DOI: 10.1201/9781003215226-38

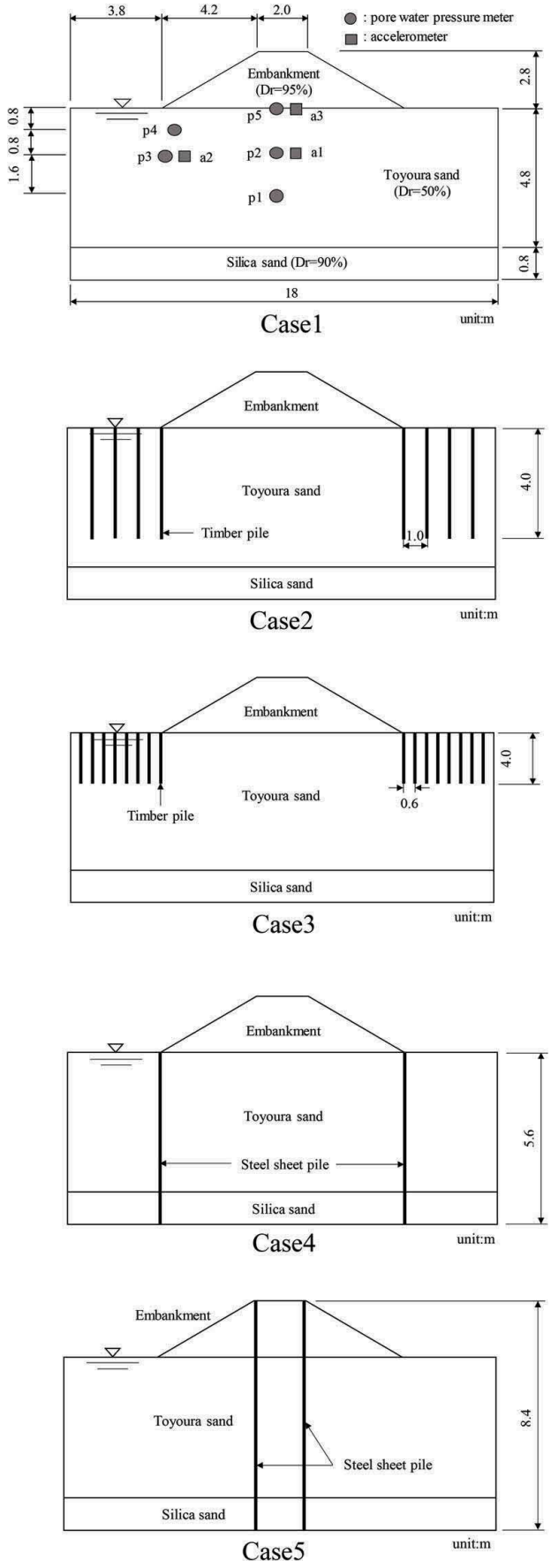

Figure 1. Research model.

wooden piles placed at 1m intervals, Case3: 2mwooden piles placed at 0.6m intervals, Case4: Penetration of the steel sheet pile from the top of the embankment to the base layer, Case5: Penetration of the steel sheet pile from the slope of the embankment to the base layer). Regarding the placement position of wooden piles, considering the workability for existing river embankments, the construction method that penetrates only the horizontal ground around the embankment is considered. The extraction points of the results in all models of displacement, pore water pressure, and horizontal acceleration are shown in Case1.

2.2 *Liquefaction experiment by dynamic centrifuge*

The liquefaction experiment is performed using the centrifuge force model test equipment owned by our school. Figure 2 shows the centrifuge model test equipment. The experimental soil layer is placed on the shaking table, the centrifugal force is loaded, and then the seismic waves are loaded to the experiment.

Table 1 shows the experimental condition, Table 2 shows physical properties (Hashida (2016)), Figure 3 shows experimental soil layer and Figure 4 shows shaking table seismic wave. In this study, the

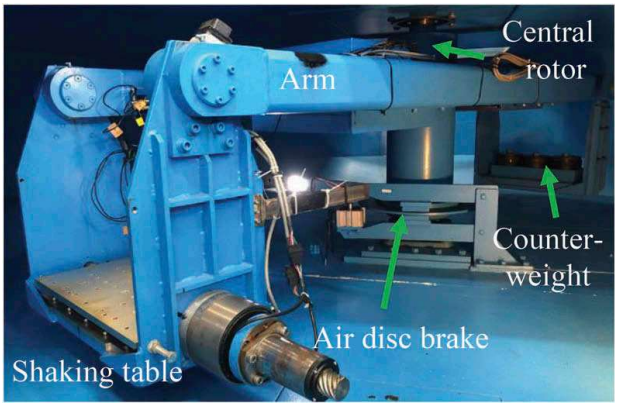

Figure 2. Centrifuge model test equipment.

Table 1. Experiment condition.

Experimental tank	Rigid earthen tank (W:455mm, H:365mm, D:140mm)
Centrifuge force field	40G
Base layer	Silica sand, Dr=95% (Air fall method)
Liquefaction layer	Toyoura standard sand, Dr=50% (Water fall method)
Embankment	Silica sand, Dr=95%
Input seismic wave	sin wave, period 20s, displacement 3mm, frequency 20Hz
Measurement items	Acceleration of in the ground and the quay Pore water pressure in the ground Settlement process and cross-sectional displacement process of back ground of sheet pile

Table 2. Physical properties of the sample.

	Unit	Embankment Silica sand (Dr=95%)	Liquefaction layer Toyoura sand (Dr=50%)	Base Layer Silica sand (Dr=90%)
Relative density (Dr)	%	95	50	90
Wet density (ρt)	g/cm^3	1.608	1.478	1.65
Maximum density (ρtmax)	g/cm^3	1.624	1.644	1.683
Minimum density (ρtmin)	g/cm^3	1.357	1.342	1.402
Volume (V)	cm^3	1508.2	7506	1251
Weight (m)	g	2425.1	11093.9	2064.2
Sand weight (ms)	g	2146.1		
Water weight (mw)	g	279		

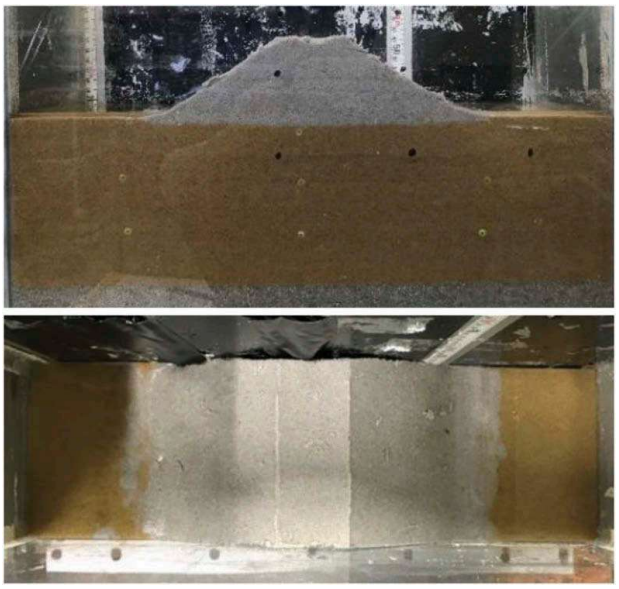

Figure 3. Case1 (before vibration).

experiment was conducted in a centrifugal force field of 40G. Also, according to the similarity rule, an experimental model size of 1/40 and groundwater using a methylcellulose aqueous solution with a viscosity of 40 mPa · s was used. The experimental soil layer was made in an experimental container with a width of 450 mm, a depth of 139mm, and a height of 355mm. The base layer was made of silica sand No. 5 with a relative density of 90%. Afterward, viscous

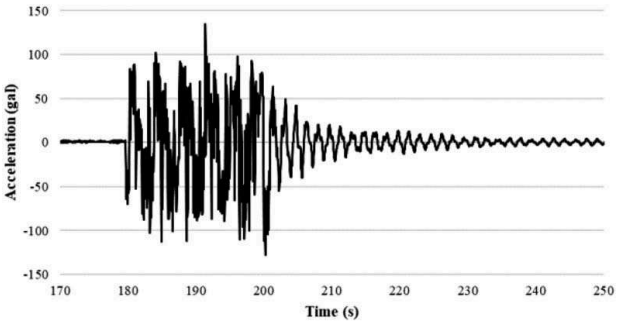

Figure 4. Shaking table seismic wave (Case1).

water was poured and a liquefaction layer was made by the underwater fall method. The liquefaction layer was made using Toyoura sand with a relative density of Dr=50%. The embankment model packed silica sand No. 7 in a dedicated formwork. After that, it is frozen, installed after the liquefaction layer is completed, and melt to make it. A wooden pile with a diameter of 5.0mm and a steel sheet pile with a thickness of 1.0mm was used. Also, the input seismic wave was tested by inputting a sine wave (frequency 20Hz, 20times, displacement 2.0mm) to the shaking table.

2.3 *Liquefaction analysis*

2.3.1 *Analysis procedure*

Liquefaction analysis is performed using the liquefaction analysis software SoilWorks for LIQCA. LIQCA is a liquefaction analysis program based on effective stress. Figure 5 shows the analysis procedure.

2.3.2 *Material parameter*

In this study, the physical property values of the ground material were determined based on the liquefaction analysis conducted by Saito (2016). Also, the liquefaction layer Toyoura sand (Dr=50%) was subjected to element simulation within Soilworks for LIQCA, and the one consistent with the results of the direct shear test conducted at our school was used (Tanimoto, W e t al. (2019)). The physical property values of steel sheet piles and wooden piles were determined from the references (Maruzen Co., Ltd. (1989), NIPPON

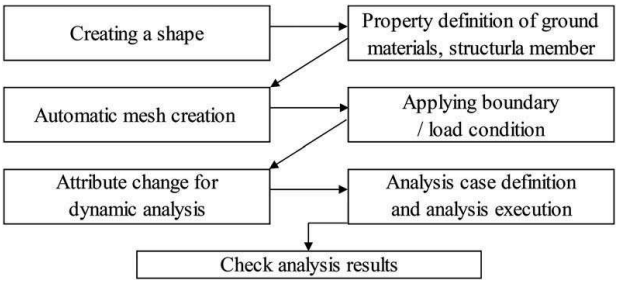

Figure 5. Analysis procedure.

STEEL CORPORATION. (2019)). Table 3 shows the physical property values of the materials used for the countermeasure work, Tables 4 and 5 show the physical property values of the ground, and Figure 6 shows the elemental simulation results of Toyoura sand (Dr = 50%).

2.3.3 *Input seismic wave*

The seismic waves used in the liquefaction analysis used the horizontal acceleration observed on the shaking table of the liquefaction experiment. Figure 7 shows the seismic waves used in the liquefaction analysis.

Table 3. Structural physical property values.

			Unit	Steel sheet pile	Timber pile
Elastic modulus			kN/m^2	205000000	100000
Unit volume weight			kN/m^2	76.44	6.860
Rigidity		Area	m^2	0.392	0.031
		Second moment of area	m^4	0.00005227	7.854
		Effective shear area ratio		0.833	0.900
		Section modulus	m^3	0.003	0.001
		Plastic section modulus	m^3	0.004	0.001
non-linear Consideration	Yield stress		kN/m^2	175000	100
	Bending moment	Mf1	kN*m	457.333	
		Mf2	kN*m	686	
	Reduction factor	a1		0.500	0.500
		a2		0.100	0.100
		a3		0.500	0.500

Table 4. Parameters for dynamic analysis.

	Unit	Embankment Silica sand (Dr=95%)	Liquefaction layer Toyoura sand (Dr=50%)	Base Layer Silica sand (Dr=90%)
Wet unit volume weight(γ_t)	kN/m^3	15.758	14.484	16.170
Satureted unit volume weight(γ_{sat})	kN/m^3	18.700	18.774	19.845
Element depth	m	1.00	1.00	1.00
Poisson's ratio		0	0	0
Static earth pressure coefficient		0	0	0
Nondimensional initial shear coefficient		873	910	1043
Initial gap ratio (e_0)		0.856	0.791	0.600
Compression exponent (λ)		0.018	0.0039	0.025
Sweling index (K)		0.006	0.00022	0.00020
Pseude-consideration ratio		1	1	1
Dilatancy factor (D_0)		5.000	0.500	0.1000
Dilatancy factor (n)		1.500	5.000	9.000
Water permeability/ Unit volume of water	$m/sec/kN/m^3$	8.67E-05	0.0001	0.0001
water volume modulus of elasticity	kN/m^2	2000000	2000000	2000000
S wave velocity	m/sec	0	0	0
P wave velocity	m/sec	0	0	0
Transformation stress ratio (M_m)		0.909	0.909	0.909
Fracture stress ratio (M_f)		1.122	1.229	1.551
Prameter in hardeining function (B_0)		2200	3500	5000
Prameter in hardeining function (B_1)		30	60	60
Prameter in hardeining function (C_f)		0	0	0
Anistropic loss parameter (C_d)		2000	2000	2000
Plasticity reference strain ($\gamma P * r$)		0.005	0.003	0.010
Elastic reference strain ($\gamma E * r$)		0.010	0.006	0.200

Table 5. Parameters for static analysis.

	Unit	Embankment Silica sand (Dr = 95%)	Liquefaction layer Toyoura sand (Dr = 50%)	Base Layer Silica sand (Dr = 90%)
Wet unit volume weight (γ_t)	kN/m^3	15.758	14.484	16.170
Satureted unit volume weight (γ_{sat})	kN/m^3	18.700	18.774	19.845
Element depth	m	1.00	1.00	1.00
Poisson's ratio		0.33	0.33	0.33
Effective soil covering pressure	kN/m^3	1.00E-08	1.00E-08	1.00E-08
Ststic earth pressure coefficient		1	1	1
Propertionality coefficient of Young's modules (E_0)		3494.07	2775.2	2775.2
Constant (n)		1	1	1
Adhesive force	kN/m^3	0	0	0
Internal friction angle (φ)		31.30	37.75	42.00

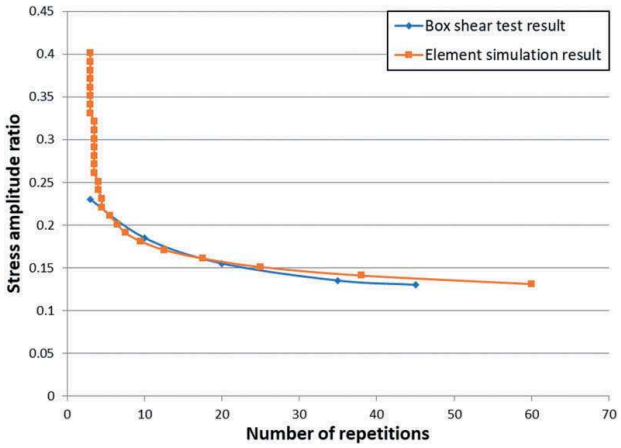

Figure 6. Element simulation.

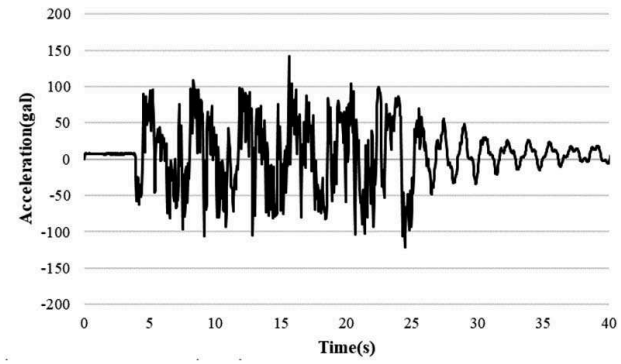

Figure 7. Input seismic wave.

2.3.4 *Analysis model*

In the liquefaction analysis, a model assuming the actual ground (hereinafter referred to as a real model) and a model assuming a liquefaction experiment (hereinafter referred to as an experimental model), two models are analyzed. The differences between these two models are the model size and boundary conditions. In the real model, the model size is increased, the sides are a cyclic boundary, and the bottom is the viscous boundary. The dimensions of the experimental model are the same as in the liquefaction experiment, and fixed boundaries are applied to the sides and bottom. The results of the real model are mainly used as the analysis results, and the experimental model is used for comparison with the experimental results. Also, the relative density increases to about 70% in the ground around the wooden piles in Case 3. Therefore, the relative density around the wooden stake is changed in the analysis model as shown in Figure 9. Figure 8 shows the schematic diagram of real model, Figure 9 shows the analysis model of Case3 and Figure 10 shows the drainage and boundary condition.

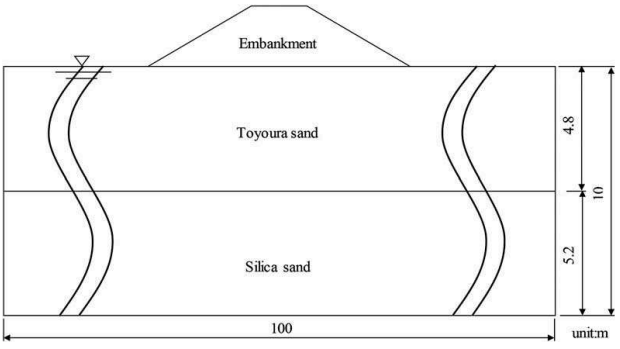

Figure 8. Real model.

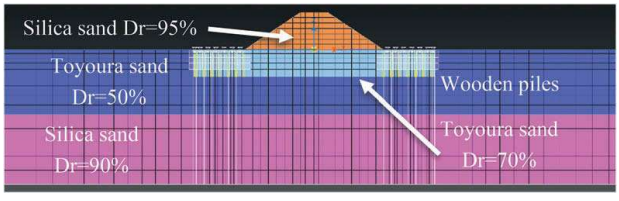

Figure 9. Analysis model (Case3).

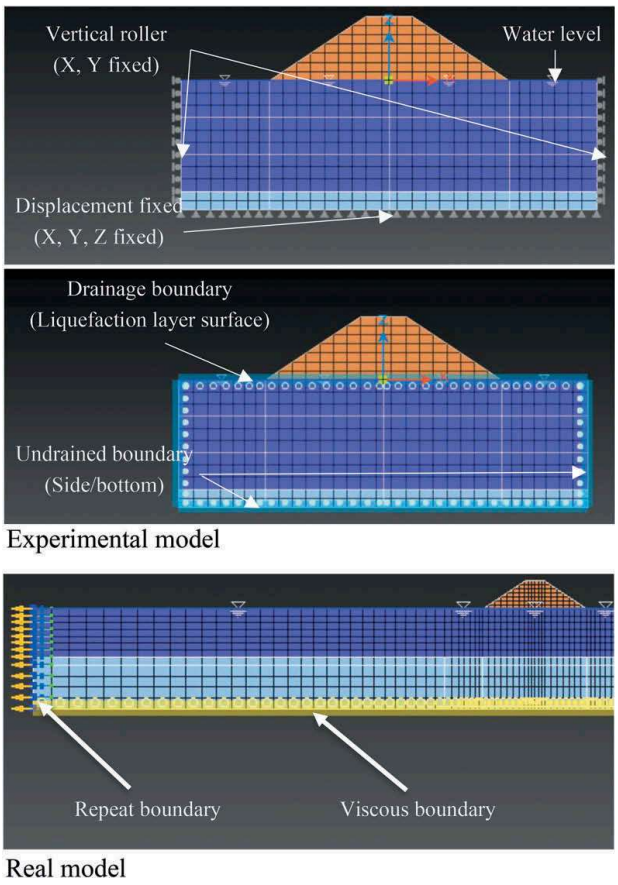

Figure 10. Drainage and boundary conditions.

3 RESEARCH RESULT

3.1 *Experimental result*

Figure 11 shows each model after shaking, and Table 6 shows the maximum displacement at each point. The values in parentheses in Table 6 show the actual displacement.

In Case1, it can be observed that the model after the experiment has variations such as the settlement of the supporting ground, rise in water level, cracks at the top of the embankment, and the lateral flow of the embankment. From these results, it is considered that the displacement due to liquefaction at the toe of the slope of the embankment led to the destruction of the embankment. It was confirmed that unmeasured river embankments may lose their river embankment function due to liquefaction.

In the experiment in which the wooden pile was penetrated, both Case2 and Case3 showed a tendency to suppress displacement and destruction. In particular, in Case3, the settlement of the top of the embankment was suppressed by 240 mm compared to Case1, and no noticeable evidence of liquefaction was confirmed on the embankment or supporting ground after the experiment. In Case3, the penetration depth of the wooden pile is shallower than in Case2, but the pile spacing is narrow, so it is considered that the effect of increasing the density of the ground shallow layer is high. Liquefaction is a phenomenon that is particularly likely to occur in shallow areas where effective stress is low. Therefore, it is presumed that Case 3 showed a greater effect of suppressing liquefaction.

In the experiment in which the sheet pile was inserted, the tendency was confirmed to suppress displacement in both Case4 and Case5 models. In Case5, there was no noticeable destruction at the top of the embankment, and it is considered that the shape of the top of the embankment was kept by the steel sheet pile. Even if the slope runs out due to liquefaction, it is unlikely that the embankment function will be lost. On the other hand, in Case4, a larger displacement and destruction of the embankment were confirmed compared to Case5, and the steel sheet pile after the experiment showed a displacement that opened outward. From these results, it can be said that in Case4, it is not enough to place a sheet pile on the toe of the slope of the embankment to suppress the lateral flow of the embankment.

Figure 12 shows the excess pore water pressure ratio measured in the experiments of each model. In all models, it is confirmed that the excess pore water pressure ratio is significantly higher in p3 and p4 than in other measuring instruments. Measuring instrument p3 and p4 are located under the toe of the slope of the embankment. It is considered that the pore water pressure tends to rise in the toe of the slope because the restraint pressure due to the embankment load does not affect the toe of the slope part.

In Case1, the excess pore water pressure ratio reached 1.0 in both p3 and p4, confirming that complete liquefaction occurred. From this, it is important to focus on the toe of the slope of the embankment as a countermeasure against liquefaction in the embankment ground. Also, the excess pore water pressure ratio, which theoretically does not exceed 1.0, greatly exceeds 1.0 at p3 and p4. This may be since the measuring instrument sank due to liquefaction and that the water pressure exceeded the theoretical value due to the occurrence of the lateral flow of the embankment. In the model in which the wooden pile was penetrated, the increase in pore water pressure was suppressed in Case2 compared to Case1, but the excess pore water pressure ratio increased to nearly 1.0 in p4. Therefore, it can be said that the effect of suppressing liquefaction as a countermeasure is imperfect.

On the other hand, in Case3, the increase in excess pore water pressure ratio is suppressed to about 0.4 even at p4. From this, the effect of

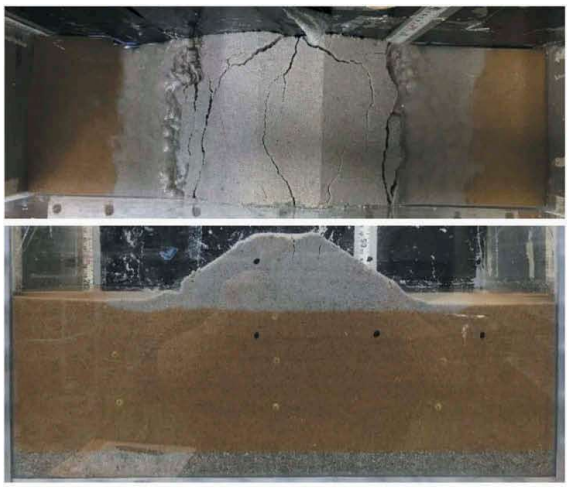

Case1

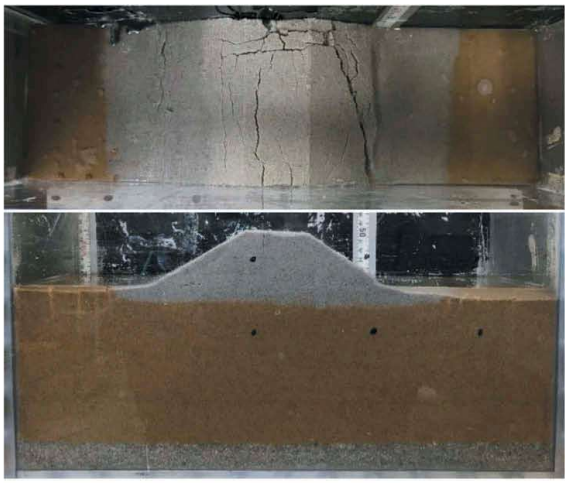

Case2

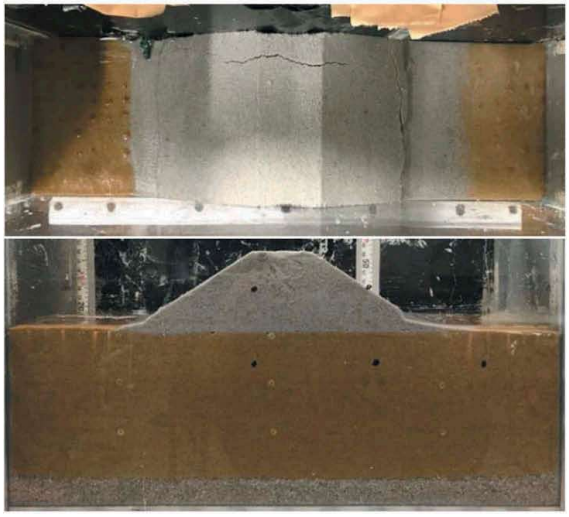

Case3

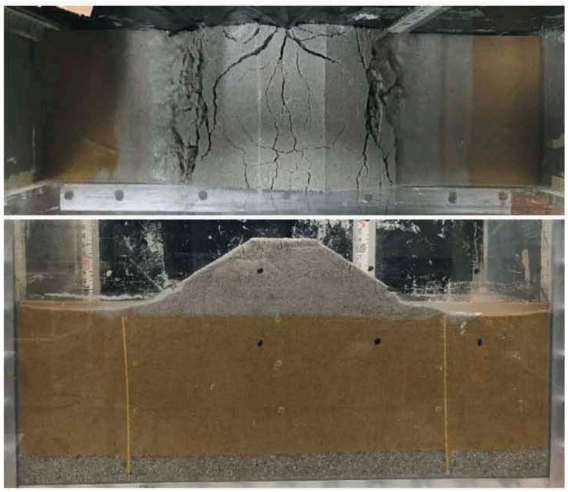

Case4

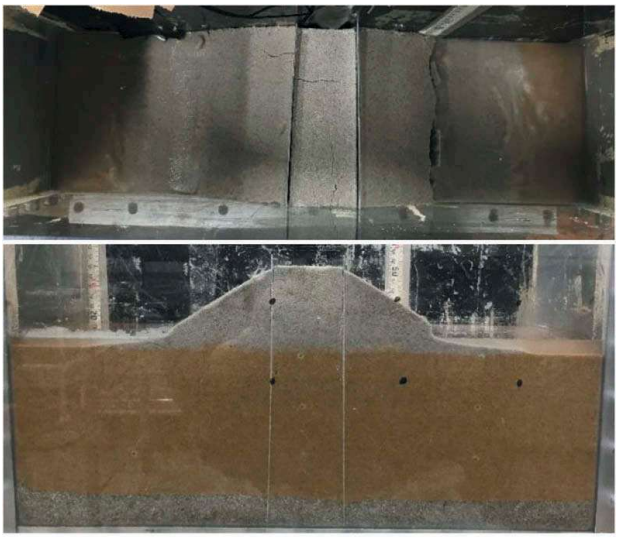

Case5

Figure 11. Observed movement.

Table 6. Maximum deformation (experimental result).

		Case1	Case2	Case3	Case4	Case5
Top of slope	displacement	6 (240)	5 (200)	1 (40)	2 (80)	2 (80)
	settlement	14 (280)	4 (160)	4 (160)	2 (80)	4 (160)
Settlement of crest		7 (280)	5 (200)	1 (40)	2 (80)	4 (160)

unit: mm

suppressing pore water pressure is great according to the dense placement of wooden piles.

In the experiment using steel sheet piles, p4 showed the highest excess pore water pressure ratio in Case4, and the numerical value was about 0.6. In Case5, it was confirmed that the excess pore water pressure ratio increased more than in Case4 in all measuring instruments. In this experiment, the steel sheet pile was inserted to the bottom of the container, the inflow and outflow of interstitial water were completely blocked.

This prevented the divergence of pore water pressure at the toe of the slope, which is also considered to be one of the reasons why the excess pore water pressure ratio exceeded Case4.

3.2 *Analysis result*

Figure 13 shows the analysis results, Table 7 shows the maximum displacement, and Figure 14 shows the excess pore water pressure ratio. In Figure 13, the red part indicates that the excess pore water pressure ratio is high. In Case1, the settlement of about 1m occurred at the top of the embankment and about 1.2 m at the bottom of the embankment. Also, it is confirmed that the embankment and the area directly below the embankment are not completely liquefied. From these results, the increase in excess pore water pressure was suppressed in the part where the suppressing pressure of the embankment was acting. It is confirmed that complete liquefaction occurs from the toe of the slope of the embankment to the horizontal ground. Therefore, it is considered that the horizontal ground part lost its bearing capacity due to liquefaction and the lateral flow was generated by the embankment load.

In Case2, the penetrated wooden piles were deformed to the extent that it was likely destruction. SoilWorks for LIQCA cannot reproduce the destruction of structural members. Therefore, in reality, the wooden piles of Case2 are expected to break. Also, the excess pore water pressure ratio is not different from Case1 at each point, and no liquefaction suppressing effect is observed.

In Case3, the lateral flow and settlement were suppressed at the toe of the slope of the embankment, so the settlement was also suppressed in the embankment. Although the excess pore water pressure ratio fluctuated sharply, it decreased by about 0.1 to 0.2 at each point compared to Case1 and Case2. From these results, it is considered that the penetration of wooden piles increased the relative density and suppressed liquefaction and displacement of the embankment.

In Case4, the amount of settlement at the top of the embankment and the amount of horizontal displacement at the bottom of the embankment were 1409 mm, which exceeded Case1. Even if the steel sheet pile was placed on the toe of the slope of the embankment, it was not possible to suppress the settlement and the lateral flow of the embankment. From Figure 13, it is confirmed that the excess pore water pressure ratio is smaller on the inside of the steel sheet pile than on the outside. It is considered that the water pressure did not increase because the steel sheet pile blocked the inflow of pore water to the area directly below the embankment.

In Case5, the settlement at the top of the embankment was most suppressed. On the other hand, the horizontal displacement of the embankment was the largest. Therefore, it can be said that the deformation of the top can be suppressed by penetrating the sheet pile into the top of the embankment, but the lateral flow of the toe of the slope cannot be suppressed. In the construction method using sheet piles such as Cases 4 and 5, the sheet pile head is deformed to open. Therefore, it is considered that deformation can be further suppressed by connecting the upper ends of the sheet pile with a tie rod.

3.3 *Comparison of analysis and experimental result*

Figure 15 shows a comparison diagram of the deformation results of the experiment and analysis. The analysis results here show the results of the experimental model. In this study, the analysis results tended to be more deformed than the experimental results. The maximum difference between the analysis results and the experimental results was about 1300 mm. The following reasons can be considered for this. (1) Suppression of deformation due to wall friction between the experimental soil layer and the container, (2) When making the embankment of the experimental soil layer, the frozen and compacted embankment was thawed and used. Therefore, it is considered to be more solid than only compressing it. (3) Consolidation of experimental soil layer by centrifugal force.

Regarding the excess pore water pressure ratio, in the experiment, there was a difference depending on the countermeasure method. But in the analysis, the same result was obtained for all models. That is

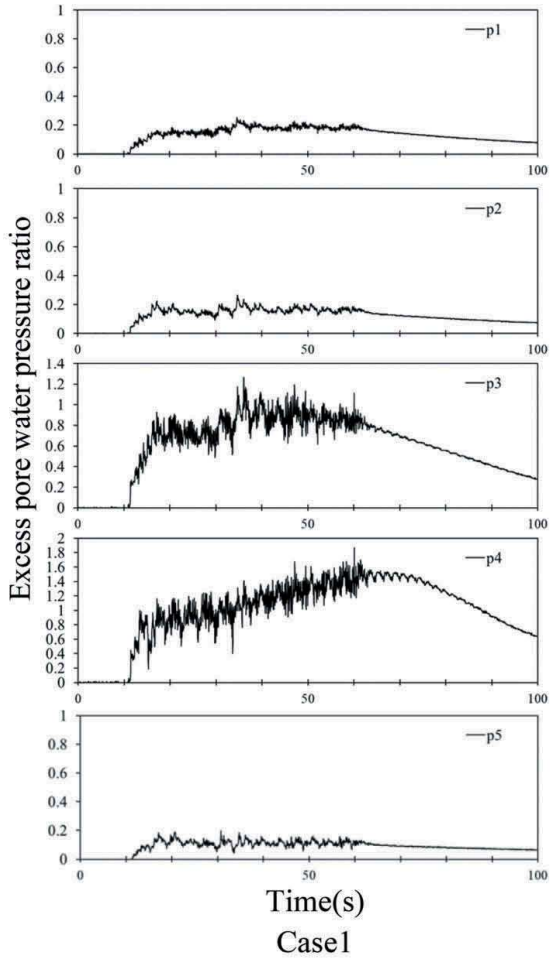

Case1

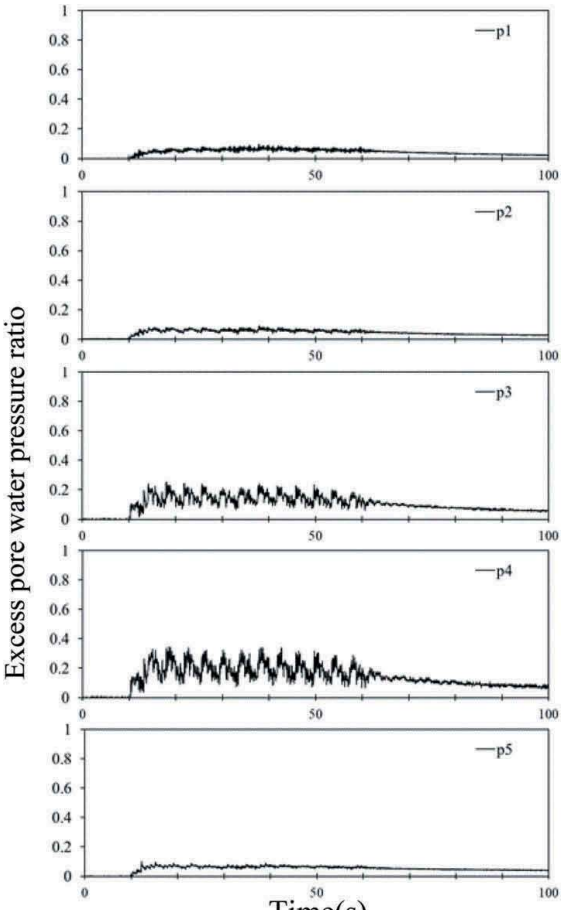

Case3

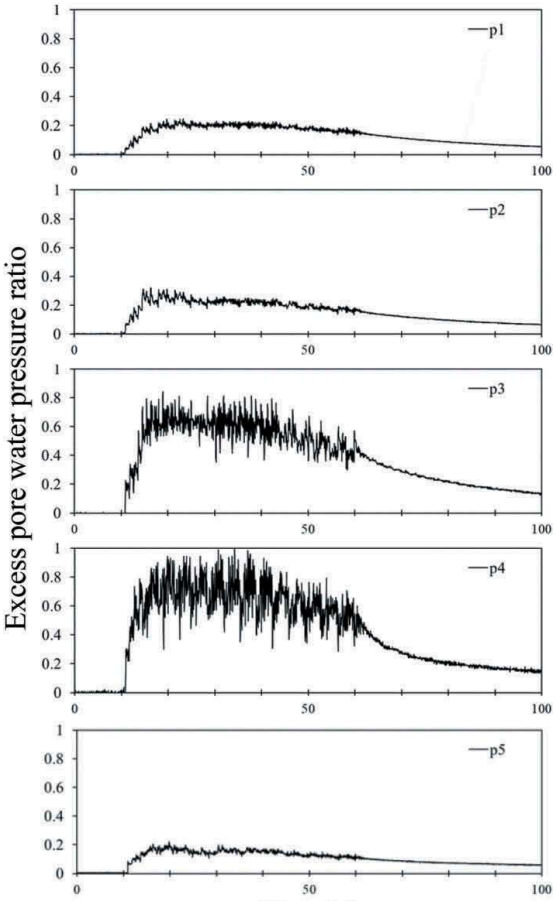

Case2

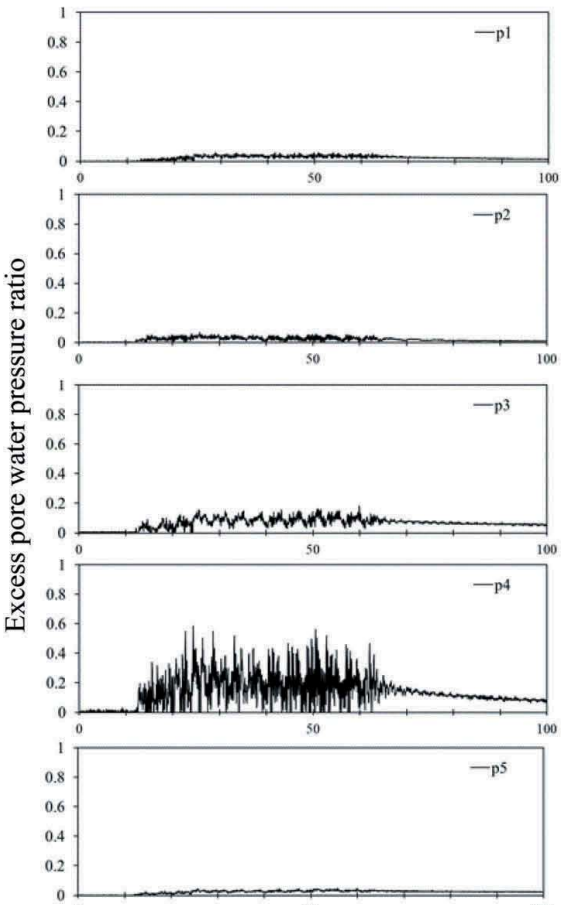

Case4

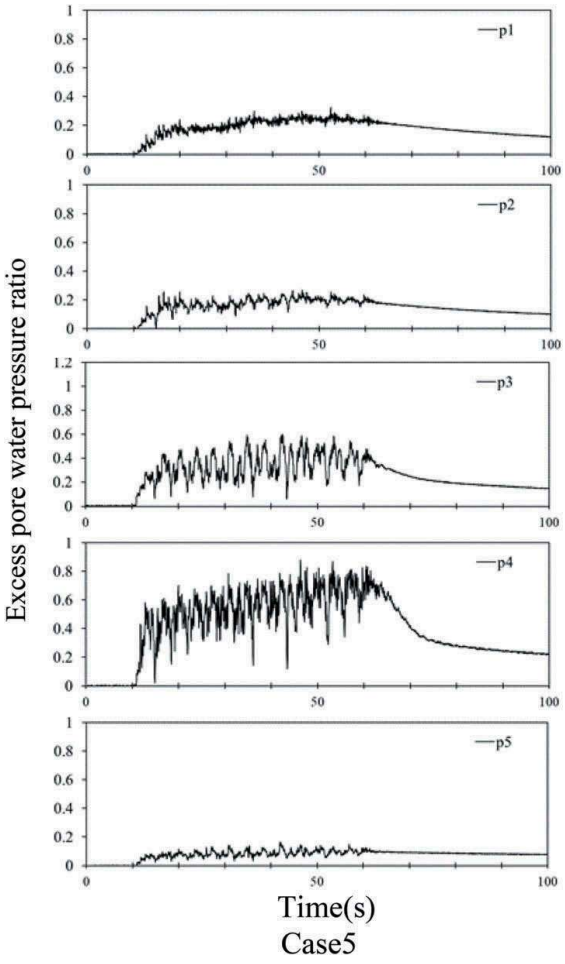

Figure 12. Time history of excess pore water pressure ratio.

(Experimental result)

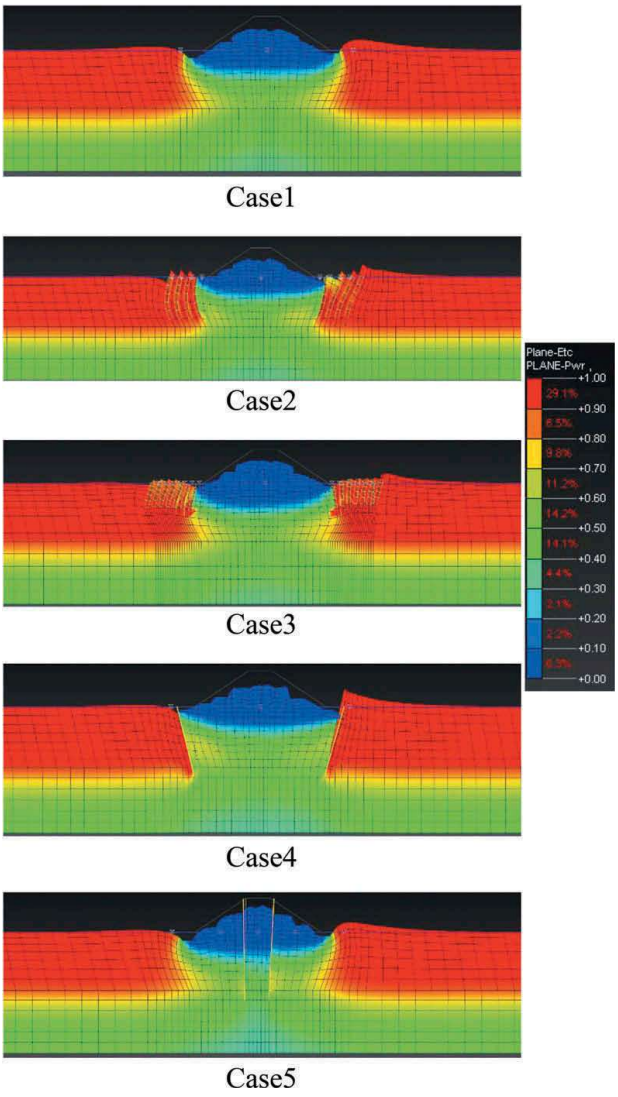

Figure 13. Analysis result.

(Displacement and excess pore water pressure ratio)

Table 7. Maximum deformation (analysis result).

		Case1	Case2	Case3	Case4	Case5
Top of slope	displacement	1279	860	856	1409	1026
	settlement	613	451	367	515	725
Settlement of crest		1045	878	851	1062	811

unit: mm

considered to be related to the physical property values of the ground material used in the analysis. In this study, element simulations have not been confirmed for ground materials other than Toyoura standard sand, which is a liquefaction layer. It is necessary to further confirm the consistency of the physical property values of the ground material in the analysis. Also, since the seismic wave used in the analysis of this study is about 40 seconds, it is considered that the behavior after the end of the earthquake cannot be sufficiently reproduced. Therefore, it is necessary to perform the analysis in a sufficient time after the principal shock is completed.

4 CONCLUSION

In this study, a method using wooden piles and sheet piles was examined as a method for suppressing liquefaction of river embankments. The findings obtained in this study are shown below.

(1) Deformation and destruction of the supporting ground and embankment were confirmed in the unmeasured river embankment. Also, liquefaction and the lateral flow occurred from the toe of the slope to the horizontal ground, leading to subsidence of the embankment. It was confirmed that there is a risk of loss of embankment function due to liquefaction of the river embankment.

(2) Deformation and excess pore water pressure ratio was suppressed by the liquefaction countermeasure method using wooden piles. In particular, it

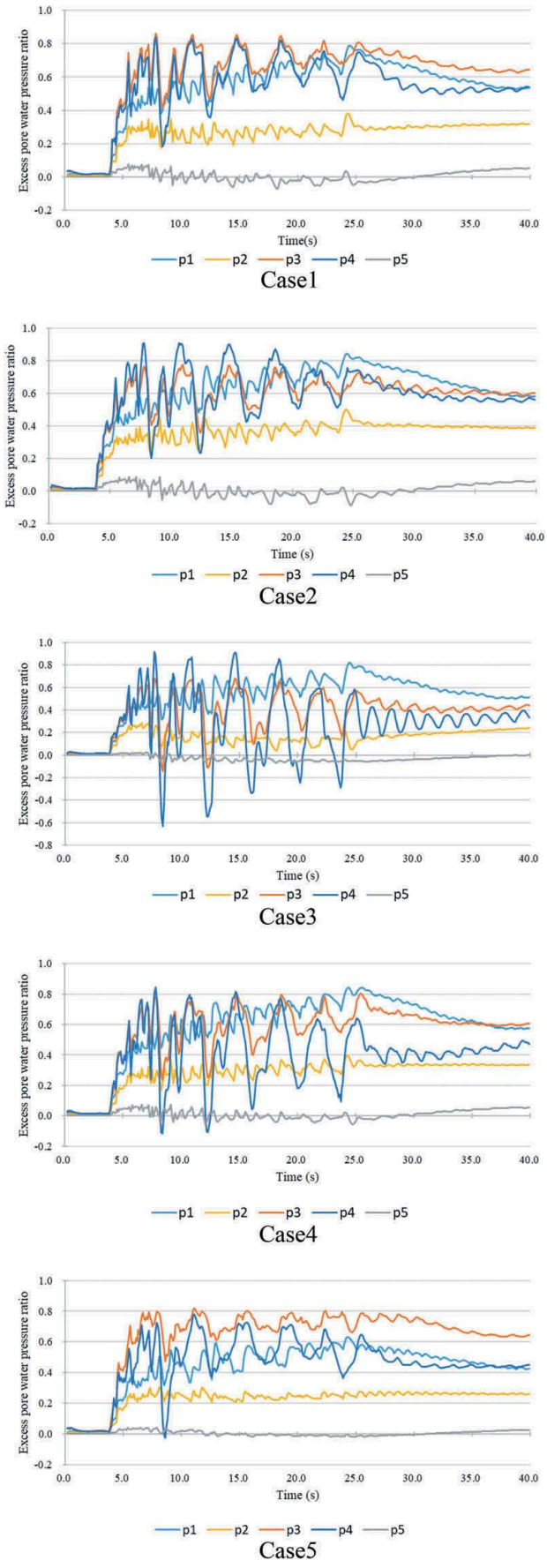

Figure 14. Excess pore water pressure ratio. (Analysis result)

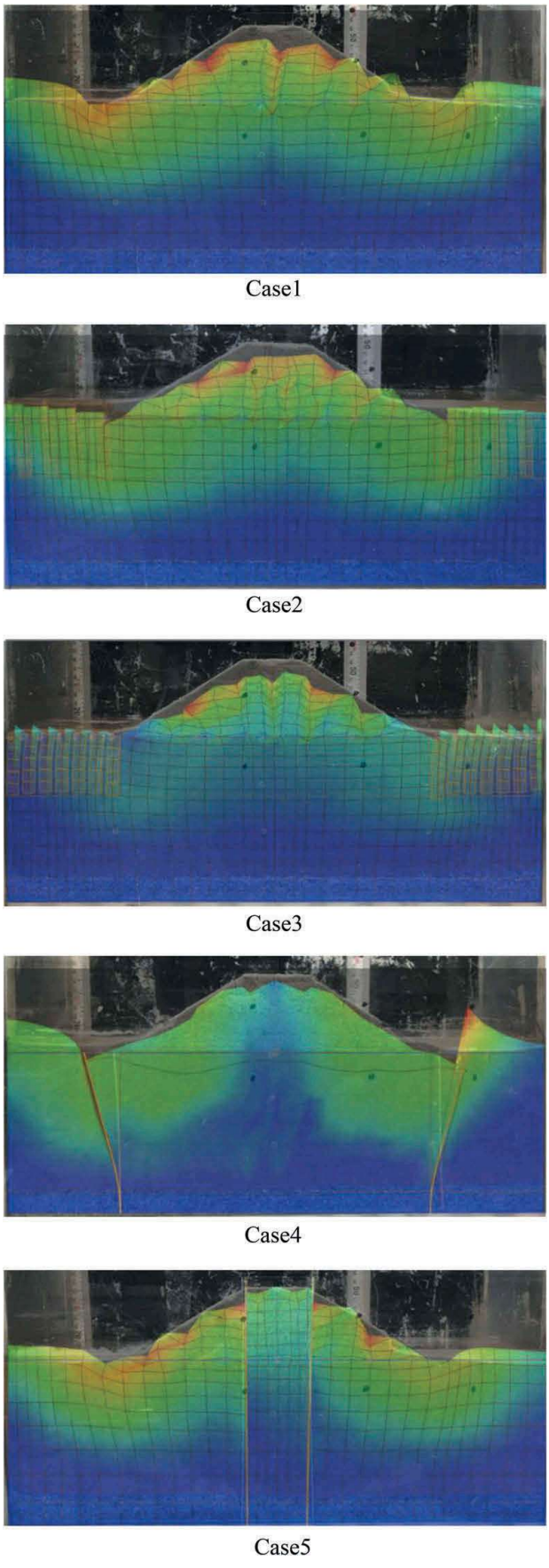

Figure 15. Displacement result comparison.

can be said that the effect was remarkable in Case 3 in which wooden piles were penetrated into the shallow layer. Therefore, it can be said that the method of increasing the ground density using wooden piles is effective as a countermeasure against liquefaction of river embankments.

(3) In Case4, where a steel sheet pile has penetrated the top of the embankment, deformation and settlement of the top of the embankment were suppressed. In the experiment, the increase in excess pore water pressure ratio was suppressed. In Case 5, where the sheet pile has penetrated the toe of the slope of the embankment, deformation on the slope of the embankment was decreased, but it was confirmed the deformation of the steel sheet pile due to the settlement of the embankment. Case4 is effective for reinforcement at the top of the embankment, and Case5 is effective for reinforcement of the slope. Also, the penetration of the sheet pile into the river embankment must do not damage the embankment and be performed in a confined construction space, so the press-in method with a static load with less vibration is considered to be suitable.

(4) Comparing the analysis results and the experimental results, a large difference was found in the deformation of the model. In the liquefaction experiment, deformation is considered to be suppressed depending on the soil layer construction method and experimental conditions. It is also necessary to improve the consistency of the ground material used for the analysis.

From the results, the effect of liquefaction countermeasures was confirmed for the construction method using wooden piles and steel sheet piles in river embankments. It can be said that the construction of wooden piles is more effective in suppressing liquefaction by narrowing the pile spacing rather than increasing the penetration depth. It was confirmed that the construction method using steel sheet piles is effective in suppressing deformation. Also, it is necessary to consider the flow of pore water in the construction method using steel sheet piles.

REFERENCES

Hashida, K. 2016. Development of dynamic centrifugal force model experimental device and research on oscillating earth pressure and embankment experiment. *Kochi National College of Technology Graduation Thesis Collection No.15* . 9-16

Japan Meteorological Agency. 2020. Information related to the Nankai Trough earthquake. https://www.data.jma.go.jp/svd/eew/data/nteq/index.html

Kochi City. 2015. Kochi City New Government Building Implementation Design [Summary Version]. *Kochi City New Government Building Construction Office*. 17

Kochi Prefecture. 2013. [Kochi version] Calculation results of damage estimation due to Nankai Trough giant earthquake (Drawing collection). *Kochi Prefecture Crisis Management Department Nankai Trough Earthquake Countermeasures Division Public materials.* 20-31

Ministry of Land, Infrastructure, Transport and Tourism. 2011. Damage and restoration status of river and coastal facilities in the Great East Japan Earthquake. *Materials provided by the River Department, Tohoku Regional Development Bureau, Ministry of Land, Infrastructure, Transport, and Tourism* . 2-46

Nakazawa, Y. 2018. Seismic response analysis and dynamic centrifuge model test on river embankment reinforcement method. *Kochi National College of Technology Graduation Thesis Collection.* 4-5

NIPPONCORPORATION STEEL. 2019. Steel sheet pile. 7 *https://www.nipponsteel.com/product/catalog_download/pdf/K007.pdf*

Tanimoto, W., Okabayashi, K., Mukaidani, M., and Hama, K. 2019. Comparison of Kochi College type cyclic box shear apparatus with cyclic triaxial apparatus. *Reiwa 1st Japan Society of Civil Engineers National Convention 74th Annual Scientific Lecture* . 2162-311

YONDEN CONSULTANTS co., Inc, Saito. 2016. Simulation analysis of centrifugal force model experiment using liquefaction analysis program LIQCA. 14

Maruzen Co., Ltd. 1989. National Astronomical Observatory of Japan, Science Chronology, 1990, Vol. 63. 444